East European Journal of Physics. 4. 635-639 (2025)
DOI:10.26565/2312-4334-2025-4-67 ISSN 2312-4334

CALCULATED FORBIDDEN BANDGAP OF Si_3MnS PHASE IN SUPERCELL (1X1X3) AND EXPERIMENTALLY DETERMINED FORBIDDEN BANDGAP OF Si<MnS>

Sh.B. Utamuradova, Sh.Kh. Daliev, A.Sh. Mavlyanov*, F. Yuldashev
Institute of Semiconductor Physics and Microelectronics at the National University of Uzbekistan, 20 Yangi Almazar st., Tashkent
**Corresponding Author e-mail: aziz.mavlon73@gmail.com*
Received July 2, 2025; revised November 11, 2025; in final form November 13, 2025; Accepted November 20, 2025

The paper presents the results of a quantum chemical calculation of a hypothetical *Si_3MnS* structure representing a "hybrid" of the cubic lattice of silicon *Si* and sphalerite *ZnS*. The *Si* lattice with a diamond structure, scaled up to a supercell (1X1X3), has been chosen for further study and calculation. Several assumptions have been made regarding the most likely substitutional sites for S and Mn impurity atoms in the Si crystal lattice. The corresponding *Si_3MnS* phase is expected to form in the first coordination shell. For quantum chemical calculations, the *Quantum ESPRESSO* suite for first-principles electronic-structure calculations and materials modeling has been adopted. The calculated forbidden bandgap of *Si_3MnS* phase in a (1X1X3) supercell turns out to be *1.14 eV*. Also, the current-voltage characteristics of *Si<Mn,S>* samples with *p-n* junction have been measured by applying the technique of temperature scanning at two comparatively low and nearly adjacent temperatures with the aim to determine the experimental forbidden bandgap energy value. The original *n*-type single-crystal silicon (phosphor-doped, specific resistance 100 Ω·cm) and p-type single-crystal silicon (boron-doped, specific resistance 1 Ω·cm) were used as initial materials for the experiments. An attempt has been made to perform a comparative analysis of forbidden bandgap values determined both during quantum-chemical calculations of the density of electronic states of the Si3MnS phase and during experimental measurements. Thorough quantum chemical calculations of IV/III-V and IV/II-VI-type "hybrid" structures in the cubic lattice of silicon and experimental measurements could incidentally shed light onto the possibility of engineering high-performance structures for future solar cells based on single crystal silicon.
Keywords: *Silicon; Hybrid Structure; Semiconductor; Current-voltage characteristics; Forbidden bandgap; Cubic Lattice*
PACS: 61.82.Fk, 61.72.Vv, 61.72.Tt, 71.20.Nr, 31.15.Ct, 31.15.−p, 31.15.Ne

INTRODUCTION

Targeted engineering of chemical molecules from a small number of defects with an ordered arrangement of impurity atoms and the atoms of the basic material in the lattice, with a partially ionic and partially covalent nature of bonds between them, could help to extend functional properties of semiconductor structures and thus vary their properties [1].

In particular, one of the promising areas is harnessing the functional properties of single crystalline silicon with non-isovalent compounds in the crystal lattice (*$Si_2A_{II}B_{VI}$* -type), representing a "hybrid" of the cubic lattice of silicon *Si* and sphalerite *ZnS* (cubic modification).

Theoretical studies, quantum chemical calculations, and experiments focused on engineering a novel class of hybrid chemical complexes with a cubic diamond-structured lattice that consists of elements of groups *IV/III-V* and *IV/II-VI*, are conducted at leading universities and research centers around the world. In particular, in [1, 2], the possibilities of nonequilibrium growth of complexes of *Si-IV/III-V* and *Si-IV/II-VI* -type compounds to obtain optically sensitive materials based on *Si* have been described. In [2,3] the authors suggest that the "hybrid" phases of *Si_2AlP* (or *Si_2ZnS*) with lattice constants close to the lattice constant of the base matrix might be ideal materials with controlled local chemical order around *Si* atoms. In all the above-mentioned studies using first-principles calculation methods, the authors discuss how chemical order impacts the electronic and optical properties of non-isovalent solid solutions. The authors in the above-mentioned papers further demonstrated, that the decomposition of the *Al-P-Si3* units leads to the formation of *Si_3AlP* containing *Al-P* "chains" as a new structural motif, as well as the *Al-P* pairs. The synthesized *Si_3AlP* shows higher absorption than bulk material of *Si* in the visible range, however the intensity of absorption is substantially lower than the theoretical result for the models based on the *Al-P* pairs.

In this regard, this paper deals with modelling and quantum-mechanical calculation of a hypothetical *Si_3MnS*-structure which is similar to the cubic structure *F43m-β-MnS* (zinc blende). The reason behind choosing for quantum-chemical calculations *Si_3MnS* was that, rich polymorphism and interesting physical properties have prompted many laboratories to study *MnS* nanocrystals in view of their possible application as photoluminescent components, catalysts, as anode material for lithium-ion batteries, and also as supercapacitors [4]. Also, in *β-MnS*, ions of S^{2-} form an *FCC* lattice, while Mn^{2+} ions occupy half of the tetrahedral voids. The ionicity of constituents in *β-MnS* phase was documented in the Materials Project international database. Thus, for further theoretical studies and calculations, a hypothetical cubic *Si_2MnS* structure of *F43m - β -MnS* space group has been chosen. For natural experiments *Si<MnS>* samples were studied. However, no ultimate objective was set to perform a comparative analysis between the results of quantum chemical calculations and the experimental results, besides some careful attempts to compare the calculated and experimentally measured forbidden bandgaps.

Cite as: Sh.B. Utamuradova, Sh.Kh. Daliev, A.Sh. Mavlyanov, F. Yuldashev, East Eur. J. Phys. 4, 635 (2025), https://doi.org/10.26565/2312-4334-2025-4-67

MATERIALS AND METHODS

All calculations were performed using the *Quantum ESPRESSO* suit for first-principles electronic-structure modelling and calculations. Using the available quantum-chemical and molecular-dynamic methods, the *Si* lattice scaled up to a supercell *(1X1X3)* with a diamond structure with location of impurity atoms S and Mn in substitutional positions in the first coordination shell in the lattice a hypothetical diamond structure was built.

The corresponding lattice parameters $a = 5.43095$ Å, b *(A-B)* $= 2.35167$ Å, and *d(A-A)* $= 33.84026$ Å were initially set for *Si* and Mn and S atoms were positioned in lattice sites in substitutional positions so to form a cubic Si_2MnS structure of $F43m$ - β -*MnS* space group (Fig. 1)

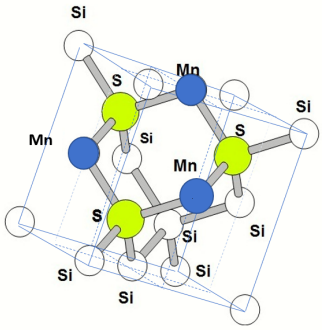

Figure 1. Cubic Si_2MnS structure of $F43m$ - β -*MnS* space group

Before the calculation, the parameters for the Si_3MnS phase in a scaled-up (1X1X3) supercell were entered (Table 1), after which the Quantum ESPRESSO software package built a phase model, representing a scalable cubic *Si* structure scaled up to (1X1X3) supercell with a single atoms of *Mn* and *S* in substitutional positions in the first upper coordination shell (Fig.2).

Table 1. Parameters of Si_3MnS-phase in the scaled-up (1X1X3)-supercell

Parameters	Phase
	Si_3MnS
a	5.46873e+00
b	2.18749e+01
c	5.46873e+00
degauss	1.00000e-02
ecutrho	4.55000e+02
ecutwfc	4.50000e+01
ibrav	8
nat	33
nbnd	141
nspin	1
ntyp	3
occupations	"smearing"
smearing	"gaussian"

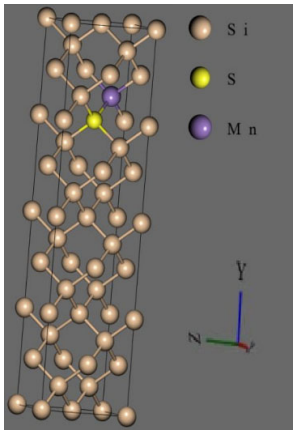

Figure 2. Si_3MnS phase in *(1X1X3)* supercell group *Fd 3m*

Of all the above parameters of ultimate interest was the parameter *"smearing"*. The point is: in case if the calculated silicon structure with impurities would have been regarded as non-metal, the option *"fixed"* should have been used instead of *"smearing"*. Incidentally, the authors of the present investigations have opted for *"smearing"*. Both options belong to Self-Consistent-Field (SCF) theory for convergence that solves the Schrodinger equation with either conventional Hartree–Fock (HF) molecular orbital theory or generalized Kohn–Sham Density Functional Theory methods. ibrav stands for Bravais lattice type.

In order to optimize the time and computational resources required for calculations, a semi-empirical method might be desirable due to less time and computational resources required for executing the method comparing to density functional theory (DFT). However, it worth noting that the accuracy of DFT is traditionally higher.

DFT offers much more accurate solutions of the Schrödinger equation compared to the classical Hartree-Fock method. The computational complexity of DFT is $O(N^3)$ [5-8]. For modeling and calculation of the density of electron states (DOS) and the band diagram of the *Si_3MnS* phase in the supercell (1X1X3), the capacity of the server station installed in the Uzbek-Japanese Innovation Center of Youth (*UJICY*) was used. To calculate the density of electronic states (DOS) for phase *Si_3MnS* in the supercell (1X1X3), the density functional theory (DFT) method was used in the *Quantum ESPRESSO* software package with Hubbard U correction (DFT+U). For calculations, no spin polarization of Mn^{2+} was taken into account.

Preliminarily, it was necessary to figure out whether the structure was geometrically correct. Thereafter, a relaxation calculation was performed, yielding the ionic positions in the relaxed structure. In the next step, instead of a relaxation calculation, we have chosen to perform a fixed-point self-consistent field (*SCF*) calculation for various ionic positions.

In *Quantum ESPRESSO*, a calculation='SCF' could be performed to find out the key state energy for a fixed ion position. For information, the SCF (self-consistent field) method is an iterative approach to solving the Schrödinger equation for a multiparticle system, on the basis of which many quantum chemical methods are built, the most famous of which is the Hartree-Fock method.

In the present work, the quantum chemical calculation considers the doped silicon model as a metal (i.e., the *occupations='smearing'* option is used) to achieve convergence more quickly, whereas in reality, the doped silicon is a semiconductor with certain value of the bandgap. In this case, by checking the output DOS file (the graph is shown in Fig. 2), we could extract the values needed to calculate the band gap value.

Regarding the experimental part, the initial *n*-type (silicon doped by phosphor with specific resistance 100 Ω·cm) and *p*-type (silicon doped with boron with specific resistance 1 Ω·cm) were used for the experiments. Doping with sulfur and manganese was performed by applying diffusion doping technique in vacuumed (10^{-4} bar) and sealed quartz ampoules at temperature of 1260^0C and 1200^0C, respectively, for a duration sufficient to ensure uniform doping. After doping with Mn and S, the initial silicon remained of *p*-type, but the resistivity increased to $\rho = 2.4 \cdot 10^4$ Ω·cm.

The forbidden band gap of the *p-n* junction formed on the basis of an *n*-type conductivity phosphor-doped silicon samples with initial resistivity of ρ=100 Ω·cm was measured (Fig.3).

At various temperatures, the current-voltage characteristics (CVC) of the *p-n* junction samples were measured. Their spectral sensitivity was also measured at room temperature by using an IKS-12 spectrophotometer in the visible light range. The current-voltage characteristics of the samples were measured using a DC source with a voltage of U=5V and U=12V, a multi-stage potentiometer with a resistance of 10 kΩ, while current measurements were carried out using a Rigol DM3068-type device, voltage measurements were carried out with a Mastech MS8040 device, a thermostat connected to a constant voltage source, digital temperature meter type Espada TPM10 with scale division of $\Delta t = 0.1^0$C. To prevent significant overheating of *p-n* structures, measurements were performed using short-term impulse voltages. The results of the current-voltage characteristics of samples with a *p-n* junction are shown in Fig. 3.

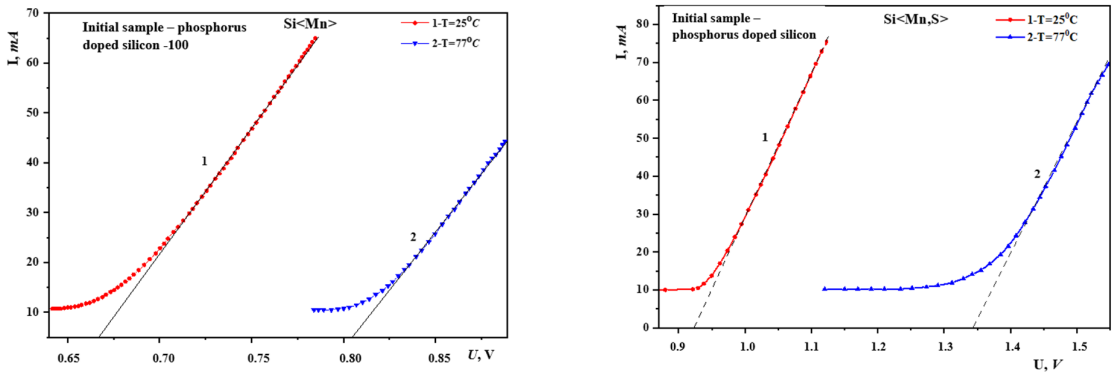

a) b)

Figure 3. Current-voltage characteristics (CVC) of silicon samples containing impurity atoms of manganese and sulfur, measured at temperatures: T= 25^0C and 2- T= 77^0C: a) Si<Mn> b) Si<Mn,S>

RESULTS AND DISCUSSION

For quantum chemical calculation of the bandgap, the *occupations='smearing'* option instead of the *occupations='fixed'* option was applied only for the reason to achieve convergence more quickly. When it comes to determining the forbidden bandgap, both options give comparatively accurate results, except for the technique of finding the forbidden bandgap from a pile of calculated databases. As the result of quantum chemical calculations by implementing the density functional theory (DFT) method, the *Quantum ESPRESSO* software suite has built the density of electronic states diagram which is illustrated on Fig.4. Based on this diagram and by checking the DOS (density of states) output file, we were able to extract the values needed to calculate the forbidden band gap.

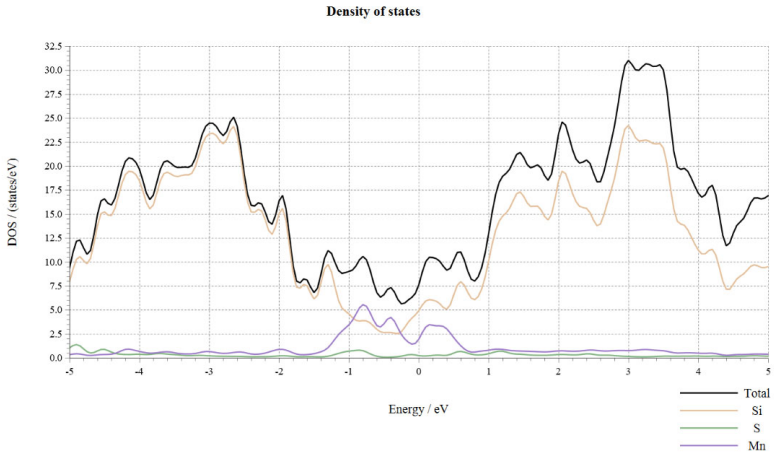

Figure 4. Density of electron states (DOS) of the Si_3MnS phase in a supercell (1X1X3) space group Fd 3m

The first line in *espresso.dos* file looks like this:

 # E (eV) dos(E) Int dos(E) EFermi = 7.049 eV

Near the Fermi level of 7.049 eV, all subsequent DOS values equal to zero were tracked. Afterwards, energy values where the first zero DOS value occurs were scanned. The first zero value appears to be 6.140 eV. Then we have scrolled up and looked for where the first non-zero DOS value appears. It appears at 7.280 eV. Incidentally the difference between these two energy values gives us the band gap value. Thus, at:

 # E (eV) dos(E) Int dos(E) EFermi = 7.049 eV

So, the bandgap of Si_3MnS phase is *(7.280 −6.140) eV=1.14 eV.*

We have also been able to determine the band gap energy of *Si<Mn>* and *Si<Mn,S>* samples, based on building temperature curve of the reverse current of the diffusive *p-n* junction. The measurements were carried out at temperatures $T = 25^0C$ and $T = 77^0C$. As a result of the measurements, the band gap value of the *Si<Mn>* sample was calculated to be 1.14 eV and that of *Si<Mn,S>* was 1.42 eV.

Tentative investigations of the short-circuit current and open-circuit voltage of *p-n*-structures, as well as the phase transitions in such structures, together with the analysis of their lux-ampere characteristic previously showed that these structures could in principle be seen as potential photodiodes and/or solar cells. Further calculations of the fill factor and efficiency ratio of these structures would pave the way for prospective application of these structures as solar cells that would allegedly extend the absorption wavelengths range. Also, as the band gap (E_g) is a core parameter of a semiconductor material, so, the authors think that an exact knowledge of the band gap in such materials makes it possible to manipulate key performance characteristics of semiconductor devices developed on the basis of such materials.

A model and results of quantum-chemical calculation of a hypothetical phase of Si_3MnS, similar to the cubic structure of *F43m-β-MnS* were proposed. The results of a comparative analysis of the bandgap value E_g of the Si_3MnS phase obtained in the process of quantum-chemical numerical calculation and the bandgap value determined during the measurement of current-voltage characteristics at two temperature points, have been compared. Preliminary geometry optimization has preceded quantum-chemical calculation of the Si_3MnS phase in supercell (1X1X3) even though as a matter of fact, frequent optimization and subsequent calculation by the density functional theory (DFT) results in the overlap of valence and conduction bands (VBM and CBM).

CONCLUSIONS

Quantum chemical calculation of the bandgap of a hypothetical Si_3MnS structure that represents a “hybrid” of the cubic lattice of silicon, Si, and sphalerite ZnS, and experimental measurements of the bandgap of *Si* samples doped with *Mn* and *S* impurity atoms have been performed. The quantum-chemical calculation yields a 1.14 eV bandgap, whereas the results of natural experiments were *1.42 eV*. The authors assume that the discrepancy between these two values may

be because, for the quantum chemical calculation, a "pristine" Si3MnS phase in a supercell (1×1×3) was used, with only *Si, Mn,* and *S* atoms in substitutional positions. In natural samples, there is a certain concentration (~10^{15}cm^{-3}) of boron atoms and oxygen atoms (~10^{17}cm^{-3}) mostly in interstitial positions. Also, larger concentrations of boron and other impurities, the absence of ideal *Si_3MnS* phases in real samples, and a variety of local irregularities in the composition and concentrations of impurity atoms in real samples, allegedly led to discrepancies in the values of the forbidden bandgaps obtained quantum chemically and experimentally.

For calculations, no spin polarization of Mn^{2+} has been anticipated, and the value of the Hubbard U parameter has not been indicated. To conduct further quantum-chemical calculations of the new "hypothetical" phases in silicon, we plan to use these parameters to improve calculation accuracy.

We assume that further in-depth theoretical studies, the detailed quantum-chemical calculations, and more thoroughly performed experiments in the field of engineering a novel class of hybrid compounds with a cubic lattice of the diamond type, where the elements of groups IV/III-V and IV/II-VI are embedded in a Si matrix, could help to forecast novel crystal structures in the future.

Meanwhile, an experimental study of the structural and electrical properties of such materials on single-crystal silicon doped with impurity atoms that theoretically form Si-IV/III-V and Si-IV/II-VI-type compounds would expand the parameter space of single-crystal silicon. It could also shed light on the potential to engineer silicon materials with closely spaced absolute minima in momentum space. In this case, it is necessary to take into account the fact that the electronic properties of such structures will differ depending on the ordered and random arrangement of impurity atoms in the silicon lattice.

ORCID

Sharifa B. Utamuradova, https://orcid.org/0000-0002-1718-1122; **Abdulaziz Sh. Mavlyanov**, https://orcid.org/0000-0003-3895-1664

REFERENCES

[1] M.K. Khakkulov, A.Sh. Mavlyanov, O.E. Sattarov, N.A. Akbarova, and Kh.K. Kamalova, "Formation of Binary Compounds of Impurity Atoms of Sulfur and Zinc in Silicon," Surface Engineering and Applied Electrochemistry, **60**(6), 826–830 (2024). https://doi.org/10.3103/S106837552470042X

[2] L. Jiang, T. Aoki, D.J. Smith, A.V.G. Chizmeshya, J. Menendez, and J. Kouvetakis, "Nanostructure-Property Control in $AlPSi_3$/Si(100) Semiconductors Using Direct Molecular Assembly. Theory Meets Experiment at the Atomic Level," Chem. Mater 26, 4092-4101 (2014). https://doi.org/10.1021/CM500926Q

[3] J. Kang, J.-S. Park, P. Stradins, and S.-H. Wei, "Nonisovalent Si-III-V and Si-II-VI alloys: Covalent, ionic, and mixed phases," Physical Review B **96**, 045203-1-045203-5 (2017). https://doi.org/10.1103/PhysRevB.96.045203

[4] Y. Tang, T. Chen, and S. Yu, Chem. Commun. **51**, 9018–9021 (2015). https://doi.org/10.1039/c5cc01700a

[5] J.A. Pople, "Quantum-Chemical Models," Advances in Physical Sciences, **132**(3), 349-356 (2002). https://doi.org/10.3367/UFNr.0172.200203f.0349

[6] B.B. Gaibnazarov, G. Imanova, Sh.T. Khozhiev, I.O. Kosimov, I.Kh. Khudaikulov, Sh.K. Kuchkanov, F.K. Khallokov and I.R. Bekpulatov, "Changes in the Structure and Properties of Silicon Carbide under Gamma Irradiation," Integrated Ferroelectrics, **237**(1), 208-215, (2023). https://doi.org/10.1080/10584587.2023.2239097

[7] K.S. Daliev, Sh.B. Utamuradova, J.J. Khamdamov, M.B. Bekmuratov, O.N. Yusupov, Sh.B. Norkulov, and Kh.J. Matchonov, "Defect Formation in MIS Structures Based on Silicon with an Impurity of Ytterbium," East Eur. J. Phys. (4), 301-304 (2024). https://doi.org/10.26565/2312-4334-2024-4-33

[8] Sh. B. Utamuradova, A. Sh. Mavlyanov, Sh. A. Sobirova, and O. E. Sattarov, "Hybrid Secondary Structure of Manganese and Sulfur in Silicon," Surface Engineering and Applied Electrochemistry, **61**(5), 633–636 (2025). https://doi.org/10.3103/s1068375525700681

РОЗРАХУНОК ЗАБОРОНЕНОЇ ЗОНА ФАЗИ Si_3MnS У СУПЕРКОМІРЦІ (1X1X3) ТА ЕКСПЕРИМЕНТАЛЬНЕ ВИЗНАЧЕННЯ ЗАБОРОНЕНОЇ ЗОНИ Si<MnS>

Ш.Б. Утамурадова, Ш.Х. Далієв, А.Ш. Мавлянов, Ф. Юлдашев

Інститут фізики напівпровідників та мікроелектроніки Національного університету Узбекистану, Ташкент

У статті представлені результати квантово-хімічного розрахунку гіпотетичної структури Si3MnS, що являє собою «гібрид» кубічної решітки кремнію Si та сфалериту ZnS. Для подальшого дослідження та розрахунку обрана решітка Si з алмазною структурою, масштабована до надкомірки (1X1X3). Було зроблено кілька припущень щодо найбільш ймовірних місць заміщення домішкових атомів S та Mn у кристалічній решітці Si. Очікується, що відповідна фаза Si3MnS утворюється в першій координаційній оболонці. Для квантово-хімічних розрахунків було використано пакет програм Quantum ESPRESSO для розрахунків електронної структури з перших принципів та моделювання матеріалів. Розрахована заборонена ширина забороненої зони фази Si_3MnS у надкомірці (1X1X3) виявилася 1,14 еВ. Також було виміряно вольт-амперні характеристики зразків Si<Mn,S> з p-n переходом, застосовуючи метод температурного сканування при двох порівняно низьких і майже суміжних температурах з метою визначення експериментального значення енергії забороненої забороненої зони. Як вихідні матеріали для експериментів використовувалися оригінальний монокристалічний кремній n-типу (легований фосфором, питомий опір 100 Ом·см) та монокристалічний кремній p-типу (легований бором, питомий опір 1 Ом·см). Була зроблена спроба провести порівняльний аналіз значень забороненої ширини забороненої зони, визначених як під час квантово-хімічних розрахунків густини електронних станів фази Si_3MnS, так і під час експериментальних вимірювань. Ретельні квантово-хімічні розрахунки «гібридних» структур типу IV/III-V та IV/II-VI у кубічній решітці кремнію та експериментальні вимірювання можуть пролити світло на можливість розробки високопродуктивних структур для майбутніх сонячних елементів на основі монокристалічного кремнію.

Ключові слова: *кремній; гібридна структура; напівпровідник; вольт-амперна характеристика; заборонена зона; кубічна решітка*